The $Co^{2+}$ or $Ni^{2+}$ statistical distribution in the B site gives rise to a distribution of the $Fe^{2+}$ ions with, on average, more $Fe^{2+}$ ions in the $Co^{2+}$- ($Ni^{2+}$-) poor regions and less $Fe^{2+}$ ions in the $Co^{2+}$- ($Ni^{2+}$-) rich regions. This would cause the different hyperfine fields at the B-site Fe nuclei.[32,33] For the Cd(II) ferrite, the area ratio (B/A) in Table I and the chemical composition (Table II) suggest that the broadening of the B line of the Mössbauer spectrum (Figure 4a) would be due to the slight oxidation of the $Fe^{2+}$ ions in the B site or due to the incorporation of some of the $Cd^{2+}$ ions into the B site (the $Cd^{2+}$ ions would be distributed in both A and B sites.)

(33) Franke, H.; Rosenberg, M. *Physica B+C (Amsterdam)* **1977**, 86-88*B+C*, 965.

**Acknowledgment.** The author wishes to thank Emeritus Prof. T. Katsura and Prof. S. Matsuo of Tokyo Institute of Technology for valuable discussions. Appreciation is also expressed to Mr. K. Fujiwara of NEC Environmental Engineering Ltd.

Contribution from the School of Chemical Sciences, University of East Anglia, Norwich NR4 7TJ, England

# Kinetics of Oxidation of the Chromium(II) Acetate Dimer by Iodine: An Example of Mixed Zero-Order/First-Order Kinetics

LADISLAV M. WILSON and RODERICK D. CANNON*

*Received January 24, 1985*

The reaction between $Cr_2(OOCCH_3)_4$ and $I_3^-$ has been studied in acetic acid solution in the presence of sodium iodide. The reaction is rapid and quantitative, and the stoichiometry corresponds to $Cr^{II}_2 + I_2 \rightarrow 2Cr^{III} + 2I^-$. The kinetics support the mechanism $Cr^{II}_2 \rightleftarrows 2Cr^{II}$ ($k_1$, $k_{-1}$), $Cr^{II} + I_2 \rightarrow$ products ($k_2$). At fixed water activity (0.4 M) and 25 °C the rate constants are $k_1 = a' + b'[NaI]^2$ and $k_2^* = k_2(k_1/k_{-1})^{1/2} = c' + d'[NaI]$ with $a' = 0.028\ s^{-1}$, $b' = 59.0\ M^{-2}\ s^{-1}$, $c' = 240\ M^{-1/2}\ s^{-1}$, and $d' = 3.18 \times 10^3\ M^{-3/2}\ s^{-1}$. The iodide dependences are attributed to an intermediate diiododichromium(II) complex $Na_2[Cr_2(OOCCH_3)_4I_2]$.

## Introduction

In previous studies, Cannon[1,2] and Stillman[2] have shown that the dimeric chromium(II) acetate reacts with a variety of oxidizing agents in one-electron steps, preceded by dissociation of the dimer into mononuclear chromium(II) species

$$Cr^{II}_2 \underset{k_{-1}}{\overset{k_1}{\rightleftharpoons}} 2Cr^{II} \quad (1)$$

$$Cr^{II} + X \xrightarrow{k_2} Cr^{III} + \text{products} \quad (2)$$

In these equations, $Cr^{II}_2$ and $Cr^{II}$ denote $Cr_2(OOCCH_3)_4$ and $Cr(OOCCH_3)_2$, with additional coordinated solvent and $CH_3CO^-$ ions, according to conditions. Two limiting rate laws have been observed, eq 3 and 4, according to whether step 1 or step 2 is rate-determining

$$R = -d[Cr^{II}_2]/dt = k_1[Cr^{II}_2] \quad (3)$$

$$R = -d[Cr^{II}_2]/dt = k_2(k_1/k_{-1})^{1/2}[Cr^{II}_2]^{1/2}[X] \quad (4)$$

In the previous experiments,[2b] the oxidizing agents X were usually taken in excess over chromium(II), but preliminary observations suggested that, with chromium(II) in excess, varieties of kinetic behavior could be observed intermediate between pseudo zero and pseudo first order, the character of the rate law varying from one to the other in a given experiment, as the concentration of oxidant X decreased with time. We have found this to be true, using iodine as oxidant and using a nonaqueous solvent to minimize the overall dissociation of the dimer (eq 1). We report here the kinetics of the reaction.

## Experimental Section

Acetic acid was dried by refluxing over boron triacetate and distilled.[3] All nitrogen used for degassing was deoxygenated by passage through BASF R3-11 catalyst. Reagent solutions were stored and mixed in vessels of the type shown in Figure 1. Iodine and chromium(II) concentrations were determined immediately before mixing in the stopped-flow apparatus, and water concentrations were determined in the mixture, after reaction. Iodine was determined by thiosulfate titration after dilution with water, chromium(II) by direct visual titration with iodine, and water by the Karl Fischer method.[4] Measured water concentrations were converted to activities by using data of Hansen et al.[5]

Chromium(II) acetate solutions were prepared by dissolving $[Cr_2(OAc)_4(OH_2)_2]$[6] in glacial acetic acid. Solutions up to about 10 mM were obtained at first, but when they were allowed to stand over several weeks, brown crystals of formula $[Cr_2(OOCCH_3)_4]\cdot 2CH_3COOH$ were deposited and the concentration fell to $[Cr^{II}_2] = 7.2$ mM. Solutions diluted with acetic acid obeyed Beer's law down to $[Cr^{II}_2] \leq 0.1$ mM. All other reagents used were analytical grade. All stopcocks were PTFE, and all solutions were handled in gas-tight syringes with PTFE plungers and needles.

Kinetic measurements were made in the HI-TECH SF-3 stopped-flow apparatus with an MCS-1 data acquisition and processing system. To avoid oxygen diffusion into the PTFE mixing system the thermostated water bath and air spaces were flushed continuously with nitrogen. To avoid stray-light effects[7] the instrument was calibrated by using solutions of iodine and NaI in acetic acid, at typical concentrations used in the kinetic studies, and at the same wavelengths and slit widths, the true transmittance being determined in separate measurements on a UNICAM SP8-200 spectrophotometer at 1-nm bandwidth. The dead time of the apparatus was estimated to be 1.5 ms (see below, Figure 7).

## Results

**1. The $I_2 + I^-$ Equilibrium.** A spectrophotometric study ($\lambda$ = 410 nm) of the equilibrium[8]

$$I_2 + NaI \overset{K}{\rightleftharpoons} NaI_3 \quad (5)$$

(1) Cannon, R. D. *J. Chem. Soc. A* **1968**, 1098.
(2) (a) Cannon, R. D.; Stillman, J. S. *Inorg. Chem.* **1975**, *14*, 2202. (b) *Inorg. Chem.* **1975**, *14*, 2207.
(3) Eichelberger, W. E.; La Mer, V. K. *J. Am. Chem. Soc.* **1933**, *55*, 3633.
(4) Smith, D. M.; Bryant, N. M.; Mitchell, J. J. *J. Am. Chem. Soc.* **1939**, *61*, 2407.
(5) Hansen, R. S.; Miller, F. A.; Christian, S. D. *J. Phys. Chem.* **1955**, *59*, 391.
(6) Cannon, R. D.; Gholami, M. J. *J. Chem. Soc., Dalton Trans.* **1976**, 1574.
(7) Burgess, C.; Knowles, A. "Standards in Absorption Spectroscopy"; Chapman and Hall: London, 1981; p 98.
(8) Under the conditions of these experiments NaOAc is undissociated, and the same is presumed to hold for NaI and $NaI_3$ (compare the value of $K(NaClO_4 \rightleftharpoons Na^+ + ClO_4^-) = 10^{-5.5}$ M): Bruckenstein, S.; Kolthoff, I. M. *J. Am. Chem. Soc.* **1956**, *78*, 2974.

0020-1669/85/1324-4366$01.50/0 

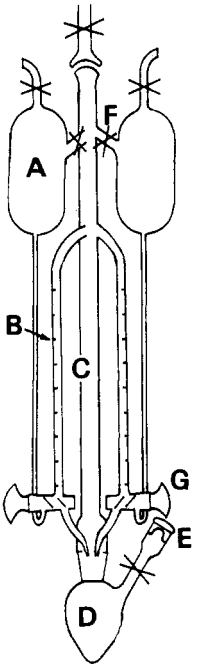


**Figure 1.** Apparatus for storing and dispensing air-sensitive solutions. There are three storage vessels A and three burets B (only two are shown here). Before the solution is withdrawn, central section C is flushed with nitrogen. Solutions are transferred via the burets to mixing flask D, mixed by magnetic stirring, and withdrawn with a hypodermic syringe (Teflon needle) through the Subaseal stopper (serum cap) E. After mixing, the burettes are left empty and the stock solutions are protected by closing the stopcocks F and G.

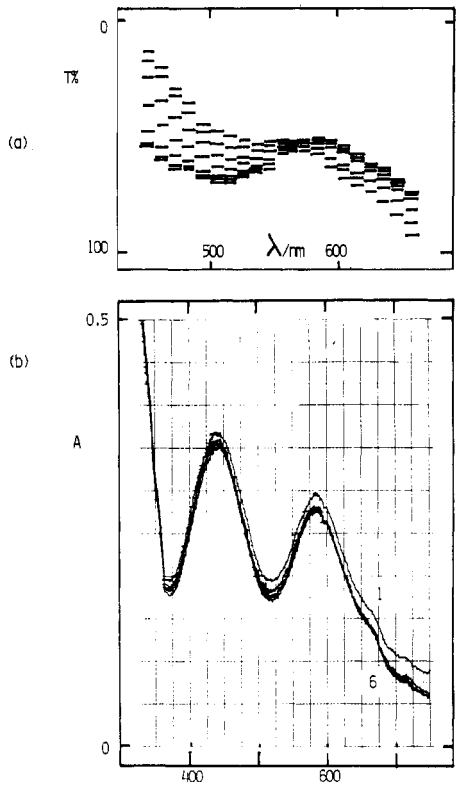


**Figure 2.** Spectral changes during the reaction $Cr_2(OOCCH_3)_4 + I_2 \rightarrow 2Cr^{III}$, in NaI solution (25 mM) in acetic acid: (a) rapid scan spectra at intervals of 0.5 s ($[Cr^{II}_2]_0$ = 4.25 mM, $[I_2]_0$ = 0.7 mM, path length 1.0 cm); (b) spectra at times (curves 1–6) $t \cong 10$ s and 1, 2, 3, 4, and 14 min ($[Cr^{II}_2]_0$ = 2.4 mM, $[I_2]_0$ = 1.5 mM. path length 1 cm).

yielded $K = (2.20 \pm 0.10) \times 10^4$ $M^{-1}$ and $(\epsilon_1 - \epsilon_0) = (6.5 \pm 0.2) \times 10^3$ $M^{-1}$ $cm^{-1}$, where $\epsilon_0$ and $\epsilon_1$ are extinction coefficients of $I_2$ and $NaI_3$, in acetic acid with $\{H_2O\}$ = 0.34 M, at 25 °C. This confirms that throughout the range of [NaI] used in our experiments the iodine is fully complexed as $NaI_3$ (apart from a few experiments mentioned in section 4 below in which the NaI concentration is initially zero).

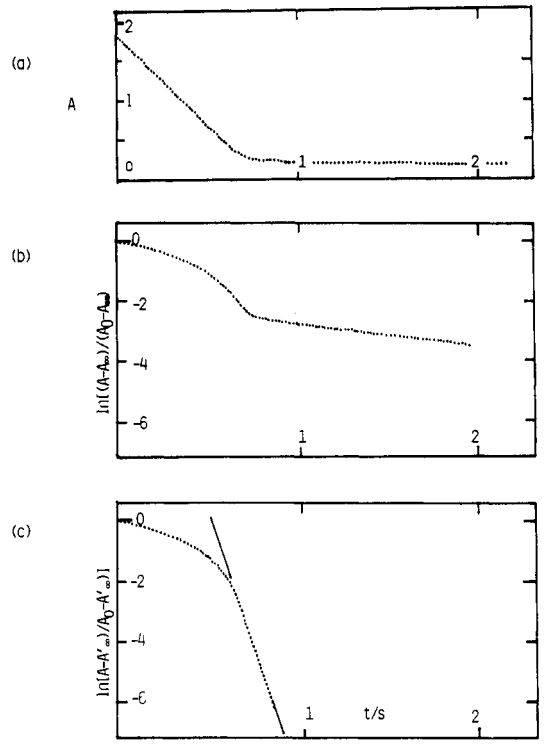


**Figure 3.** (a) Absorbance–time curve for $[Cr^{II}_2]_0$ = 5.15 mM, [NaI] = 25 mM, $[H_2O]$ = 0.15 M, and $[I_2]_0$ = 0.30 mM at 25 °C, path length 2 mm, and λ = 355 nm. The slope of the descending part gives the rate constant $k^0$. (b) Logarithmic plot of same data, using $A_\infty$ = 0.110 from part a. (c) Logarithmic plot using $A_\infty'$ = 0.218, extrapolated from Figure 5. The fitted straight line gives the rate constant $k^1$.

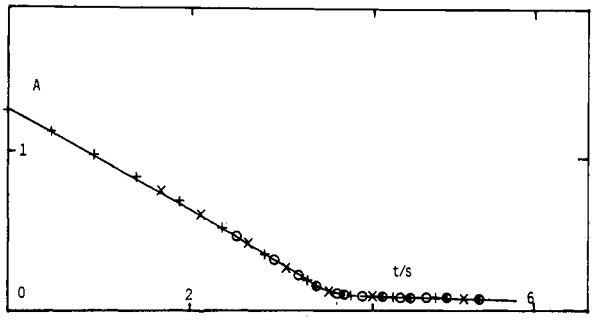


**Figure 4.** Absorption–time traces showing superimposition of curves for different initial iodine concentrations ($[Cr^{II}_2]$ = 4.25 mM, [NaI] = 25 mM, $[H_2O]$ = 0.15 M, 25 °C, path length 2 mm, λ = 410 nm). $[I_2]_0$ (mM): (+) 0.6; (×) 0.4; (○) 0.2; (◐) 0.05.

**2. The Redox Reaction: Stoichiometry and Phases.** When solutions of $Cr_2(OAc)_4$ and $I_2$ are mixed, the reaction is complete within a few seconds. Typical spectral changes are shown in Figure 2. Two phases could be distinguished clearly: (A) a rapid change to the characteristic spectrum of chromium(III), with an isosbestic point at λ ≅ 570 nm and (B) a slow decrease in absorbance at all wavelengths. The 570-nm isosbestic was observed also in reactions with $I_2$ initially in excess over $Cr^{II}_2$. The spectrum after phase A resembles that of the trinuclear basic acetate ion $[Cr_3O(OOCCH_3)_6(H_2O)_3]^+$, including the characteristic peaks at 666 and 715 nm.[9] Phase B was not investigated, except to note that it showed pseudo-first-order kinetics and was slow enough not to interfere with calculations of rates of phase A.[10]

(9) Dubicki, L.; Day, P. *Inorg. Chem.* **1972**, *11*, 1868.
(10) E.g. $k_{obsd} = -d \ln [A - A_\infty]/dt = 2.4 \pm 0.2$ $s^{-1}$ (25 °C, initial concentrations $[Cr^{II}]_T$ = 4.25 mM, $[I_2]_T$ = 0.28 mM, [NaI] = 25 mM, and $[H_2O] \cong 0.18$ M.

**3. Kinetics.**[11] In most experiments, sodium iodide was maintained in large excess over other reagents and chromium(II) was initially in excess over iodine. A typical absorbance–time curve is shown in Figure 3a. In the lower ranges of NaI and $H_2O$ concentrations, the curves show a clear division into an initial linear portion, a curved portion, and a nearly horizontal "infinite-time" portion. For various initial iodine concentrations the curves were superimposable (when shifted along the time axis), the initial linear portions becoming shorter while the curved portions remained virtually unchanged (Figure 4). At the lowest iodine concentrations used, the curvature covered the whole time span, and the same was true with higher iodine concentrations, when the iodide and water concentrations were increased. The linear and curved portions of these plots do *not* correspond respectively to the two phases of reaction shown by the scanning spectra. In general, phase A covers the linear portion and part of the curved portion, and phase B covers the later part of the curved portion. Thus the kinetics of phase A can be described as pseudo zero order with respect to iodine, changing to a higher order (in fact pseudo first order as shown below) when the iodine concentration is very small.

These kinetics are consistent with the mechanism given in eq 1 and 2, with X = $I_2$ and with the addition of the further rapid step

$$Cr^{II} + I_2^- \rightarrow\!\!\!\!\rightarrow Cr^{III} + 2I^- \quad (6)$$

Applying the steady-state condition to the intermediate $Cr^{II}$, we have

$$d[Cr^{II}]/dt = 2k_1[Cr^{II}_2] - 2k_{-1}[Cr^{II}]^2 - 2k_2[Cr^{II}][I_2] = 0 \quad (7)$$

while the overall rate of reaction is given by

$$R = -d[I_2]/dt = k_2[Cr^{II}][I_2] \quad (8)$$

Elimination of $[Cr^{II}]$ between these equations gives

$$R = 2k_1[Cr^{II}_2]/[1 + (1 + 4k_1k_{-1}k_2^{-2}[Cr^{II}_2]x^{-2})^{1/2}] \quad (9)$$

where $x = [I_2]_T$ and the limiting forms at high and low $x$ are given by eq 3 and 4, with X = $I_2$. These may be written as eq 10 and 11, respectively.

$$R = k^0 \quad (10)$$

$$R = k^1[I_2] \quad (11)$$

$k^0$ and $k^1$ are pseudo-zero-order and pseudo-first-order rate constants corresponding to the first two portions of the absorbance–time curve and the chromium(II) dependences are given by

$$k^0 = k_1[Cr^{II}_2] \quad (12)$$

$$k^1 = k_2^*[Cr^{II}_2]^{1/2} \quad (13)$$

where $k_2^* = k_2(k_1/k_{-1})^{1/2}$. Both the mechanism and the kinetics are formally analogous to the system $Mn_2(CO)_{10} + O_2$ studied by Poë and co-workers.[12] However, different methods of treatment of the data were appropriate, depending on the character of the absorbance–time plots:

(1) In the most general case, the plot of absorbance, $A$, against time, $t$, was transformed to a plot of slope, $S = -dA/dt$, against $A$, and compared with curves calculated from the equation

$$S = dA/dt = 2S_0[1 + (1 + B^2/(A - A_\infty')^2)^{1/2}] \quad (14)$$

the parameters $A_\infty'$, $B$, and $S_0$ being adjusted to give the best visual fit. A typical curve is shown in Figure 5. The parameter $S_0$ = $(A_0 - A_\infty')[I_2]_0^{-1}k^0$ is the asymptotic value of $S$ and $B = (A_0 - A_\infty')[I_2]_0^{-1}(2k^0/k^1)$ measures the curvature of the rising part. The value of $A_\infty'$ was obtained by manual extrapolation, ignoring the small "tail", which corresponds to phase B of the reaction.

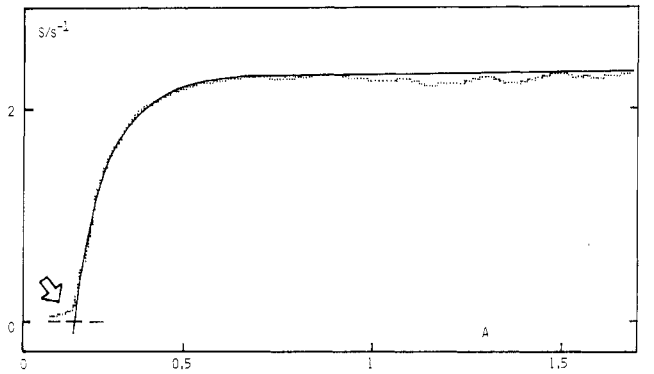


**Figure 5.** Plot of $S = -dA/dt$, against $A$, for same data as used in Figure 3. Values of $S$ were obtained by a quadratic least-squares fit to successive groups of 11 points in the curve a of Figure 3. The "tail" marked by the arrow corresponds to the onset of phase B of the reaction. The continuous curve was calculated from eq 14, with the parameters $A' = 0.218$, $S_0 = 2.41$ s$^{-1}$, and $B = 0.22$.

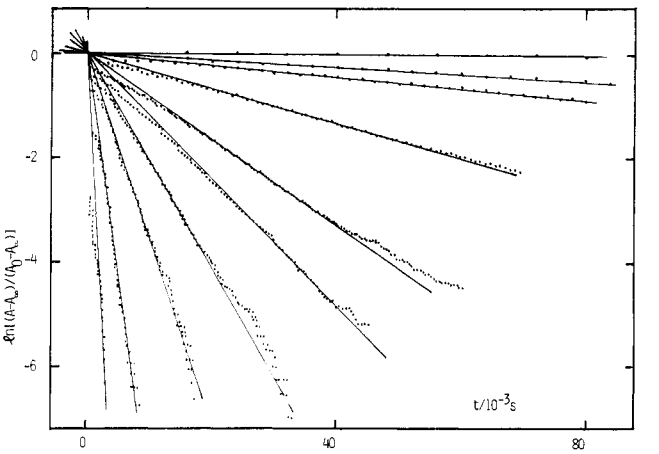


**Figure 6.** Logarithmic plots for reactions under conditions of pseudo-first-order kinetics ($[I_2]_0 = 0.10$ mM, $[Cr^{II}_2] = 2.40$ mM, [NaI] = 25.0 mM; $[H_2O] = 0.46$–11.8 M, path length 2 mm, $\lambda = 355$ nm). Straight lines fitted to the data points converge at $t \cong -1.5$ ms, the dead time of the stopped-flow apparatus.

(2) When the linear part of the $A(t)$ curve was substantial (see, e.g., Figures 3a and 4) the initial slope $S_0$ was measured directly and $k^0$ was calculated as

$$k^0 = S_0/\Delta\epsilon l \quad (15)$$

where $\Delta\epsilon$ is the extinction coefficient change for the reaction, given in turn by $\Delta\epsilon l = (A_0 - A_\infty')/[I_2]_0$ averaged over all experiments at the wavelength used.

(3) When the curved portion of the plot was substantial, $k_1$ was obtained from a graph of log $(A - A_\infty')$ against $t$, as shown in Figures 3c and 6.

Rate constants $k^0$ and $k^1$ are listed in Table I. Over the range of chromium(II) concentrations used, the first-order dependence of $k^0$, and the half-order dependence of $k^1$ (eq 12 and 13) are confirmed. (Figures 7 and 8). Both rate constants are independent of iodine concentration but increase with increasing water activity and with increasing sodium iodide concentration. Empirical rate expressions were found by fitting logarithmic plots of the data to calculated curves, as shown in Figures 9 and 10. At [NaI] = 0.025 M, the water dependences are best represented by

$$k_1 = a\{H_2O\} + b\{H_2O\}^2 \quad (16)$$

$$k_2^* = c + d\{H_2O\}^2 \quad (17)$$

(11) Throughout this paper, concentrations without subscripts refer to sums of concentrations of species with various coordinated ligands, i.e. $[Cr_2^{II}] = \sum_n[Cr_2(OAc)_4L_n]$ and $[I_2] = \sum_n[I_2L_n]$, where L may be HOAc, $H_2O$, or NaOAc; $[I^-]$ = [NaI] and $[I_3^-]$ = $[NaI_3]$. Subscripts T denote the total concentrations of the specified oxidation states, i.e. $[Cr_2^{II}]_T = [Cr_2^{II}] + \sum_n[Cr_2(OAc)_4(NaI)_n]$; $[I^-]_T$ = [NaI] + $[NaI_3]$ + $\sum_n[Cr_2(OAc)_4(NaI)_n]$; $[I_2]_T = [I_2] + [NaI]$. Subscript zeros, e.g. $[Cr_2^{II}]_0$, denote these total concentrations at time $t = 0$.

(12) Fawcett, J. P.; Poë, A.; Sharma, K. R. *J. Am. Chem. Soc.* **1976**, *98*, 1401.

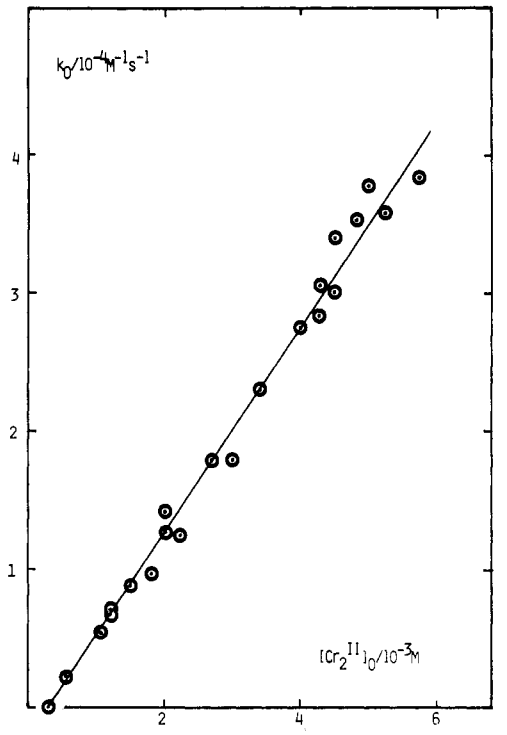


**Figure 7.** Plot of $k^0$ against $[Cr^{II}_2]_0$ ([NaI] = 25 mM). The straight line is drawn with the intercept at $[Cr^{II}_2]_0$ equal to the average of $[I_2]_0$ for the experiments.

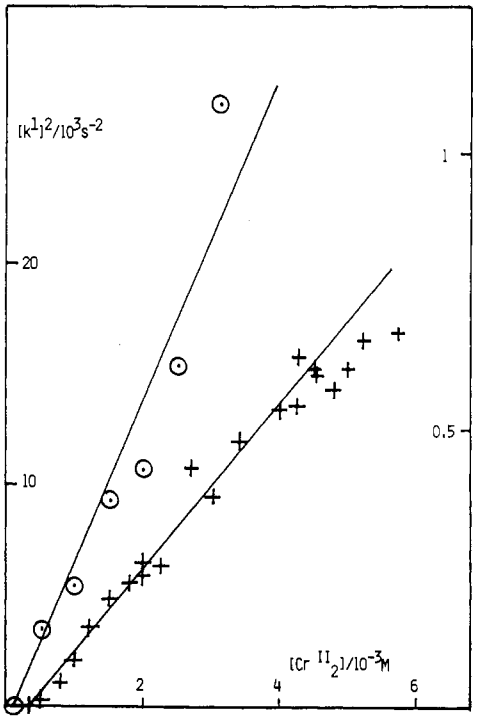


**Figure 8.** Plot of $[k^1]^2$ against $[Cr^{II}_2]_0$ (see text, eq 11 and 13): (⊙) [NaI] = 175 mM (left-hand side); (+) [NaI] = 25 mM (right-hand side). The lines are drawn with intercepts at $[Cr^{II}_2]_0 = \langle[I_2]_0\rangle$ as in Figure 7.

with $a = 0.112\ M^{-1}\ s^{-1}$, $b = 0.056\ M^{-2}\ s^{-1}$, $c = 275\ M^{-1/2}\ s^{-1}$, and $d = 132\ M^{-2.5}\ s^{-1}$. At $\{H_2O\} = 0.4$ M, the iodide dependences may be represented as

$$k_1 = a' + b'[NaI]^2 \quad (18)$$

$$k_2^* = c' + d'[NaI] \quad (19)$$

with $a' = 0.028\ s^{-1}$, $b' = 59.0\ M^{-2}\ s^{-1}$, $c' = 240\ M^{-1/2}\ s^{-1}$, and $d' = 3.18 \times 10^3\ M^{-1.5}\ s^{-1}$.[13]

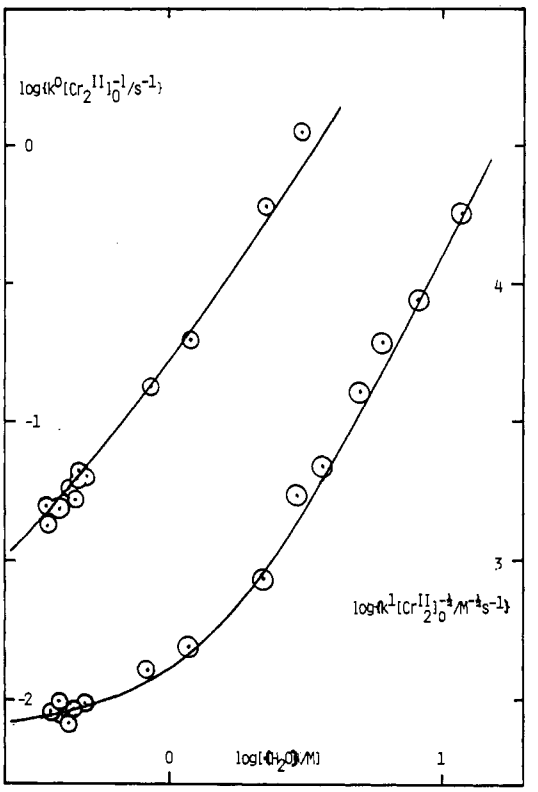


**Figure 9.** Water dependence of $k^0$ and $k^1$ ([NaI] = 25 mM). The lines are drawn with equations $k^0[Cr^{II}_2]^{-1} = a\{H_2O\} + b\{H_2O\}^2$ and $k^1 \cdot [Cr^{II}_2]^{-1/2} = c + d\{H_2O\}^2$, where $a = 0.112\ M^{-1}\ s^{-1}$, $b = 0.056\ M^{-2}\ s^{-1}$, $c = 275\ M^{-1/2}\ s^{-1}$, and $d = 132\ M^{-2.5}\ s^{-1}$.

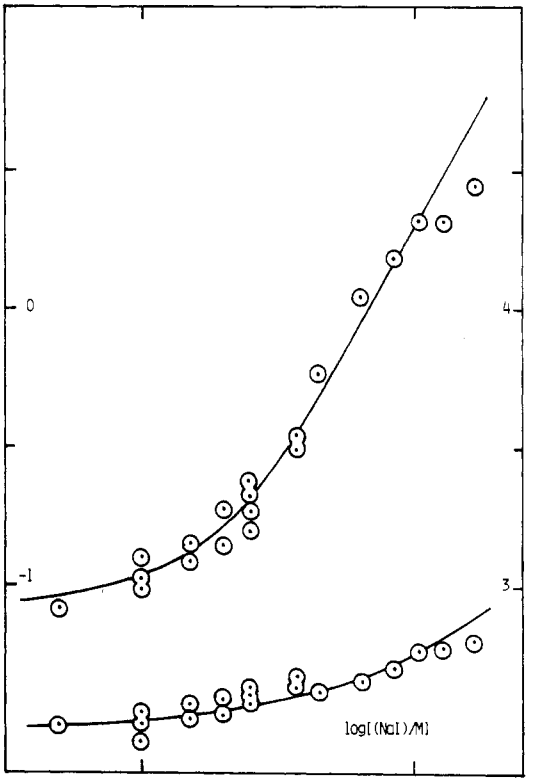


**Figure 10.** Iodide dependence of $k^0$ and $k^1$: upper curve and left-hand scale, log $(k^0[Cr^{II}_2]_0^{-1}\{H_2O\}^{-1.18}/M^{-1.18}\ s^{-1})$; lower curve and right-hand scale, log $(k^1[Cr^{II}_2]_0^{-1/2}\{H_2O\}^{-0.17}/M^{-0.17}\ s^{-1})$. See text and footnote 13. The curves are drawn according to the equations $k^0[Cr^{II}_2]^{-1}\{H_2O\}^{-1.18} = a + b[NaI]^2$, with $a = 0.083\ M^{-1.18}\ s^{-1}$ and $b = 174\ M^{-3.18}\ s^{-1}$, and $k^1[Cr^{II}_2]^{-1/2}\{H_2O\}^{-0.17} = a + b[NaI]$ with $a = 282\ M^{-0.67}\ s^{-1}$ and $b = 3.72 \times 10^3\ M^{-1.67}\ s^{-1}$.

**4. Iodide Release.** Attempts were made to determine whether or not iodide is released in the primary electron-transfer step,

**Table I.** Kinetic Data[a]

| $\{H_2O\}$,[b] M | [NaI], $10^{-3}$ M | $[I_2]_0$, $10^{-5}$ M | $[Cr^{II}_2]_0$, $10^{-3}$ M | $k^0$,[c] $10^{-3}$ $M^{-1}$ $s^{-1}$ | $k^1$,[d] $s^{-1}$ | $\{H_2O\}$,[b] M | [NaI], $10^{-3}$ M | $[I_2]_0$, $10^{-5}$ M | $[Cr^{II}_2]_0$, $10^{-3}$ M | $k^0$,[c] $10^{-3}$ $M^{-1}$ $s^{-1}$ | $k^1$,[d] $s^{-1}$ |
|---|---|---|---|---|---|---|---|---|---|---|---|
| | | | | | $\lambda$ = 410 nm | | | | | | |
| 0.45 | 25 | 28 | 4.5 | 0.301 | 24.7 | 0.45 | 25 | 28 | 2.7 | 0.179 | 20.7 |
| 0.45 | 25 | 28 | 4.0 | 0.275 | 23.1 | 0.41 | 25 | 28 | 2.0 | 0.128 | 16 |
| 0.45 | 25 | 28 | 3.4 | 0.229 | 21.8 | | | | | | |
| 0.46 | 25 | 28 | 4.25 | 0.282 | 25.1 | 0.38 | 25 | 28 | 1.2 | 0.070 | 12 |
| 0.42 | 25 | 28 | 3.0 | 0.179 | 19.4 | 0.38 | 25 | 28 | 1.2 | 0.070 | 12 |
| 0.40 | 25 | 28 | 2.24 | 0.123 | 16 | 0.34 | 25 | 28 | 1.04 | 0.053 | 9 |
| 0.40 | 25 | 28 | 1.8 | 0.096 | 14.8 | 0.34 | 25 | 28 | 0.8 | 0.037 | 6.3 |
| 0.48 | 25 | 28 | 1.5 | 0.088 | 14 | 0.31 | 25 | 28 | 0.5 | 0.022 | 3 |
| 0.53 | 25 | 36 | 5.75 | 0.384 | 26.0 | 0.53 | 25 | 36 | 4.5 | 0.340 | 24.5 |
| 0.53 | 25 | 36 | 5.22 | 0.358 | 25.7 | 0.53 | 25 | 36 | 4.25 | 0.305 | 23.3 |
| 0.53 | 25 | 36 | 5.0 | 0.378 | 24.6 | 0.53 | 25 | 36 | 2.0 | 0.141 | 15.3 |
| 0.53 | 25 | 36 | 4.8 | 0.352 | 23.9 | | | | | | |
| 0.38 | 25 | 62 | 3.62 | 0.179 | 17 | 0.47 | 25 | 110 | 3.62 | 0.235 | 18.5 |
| 0.40 | 25 | 75 | 3.62 | 0.186 | 18.8 | 0.46 | 25 | 125 | 3.62 | 0.229 | 17.2 |
| 0.40 | 25 | 75 | 3.62 | 0.178 | 15.6 | 0.48 | 25 | 140 | 3.62 | 0.235 | 18 |
| 0.44 | 25 | 90 | 3.62 | 0.205 | 17.6 | | | | | | |
| 0.35 | 25 | 5 | 4.25 | 0.165 | 15.9 | 0.40 | 25 | 40 | 4.25 | 0.211 | 17.0 |
| 0.40 | 25 | 20 | 4.25 | 0.202 | 16.1 | 0.31 | 25 | 60 | 4.25 | 0.205 | 15.5 |
| | | | | | $\lambda$ = 355 nm | | | | | | |
| 0.46 | 25 | 10 | 2.4 | 0.196 | 14.1[f] | 11.8 | 25 | 10 | 2.4 | *e* | 900[f] |
| 0.87 | 25 | 10 | 2.4 | 0.477 | 20.1[f] | 0.37 | 10 | 30 | 5.15 | 0.164 | 16 |
| 1.23 | 25 | 10 | 2.4 | 0.712 | 22.3[f] | 0.38 | 25 | 30 | 5.15 | 0.40 | 22 |
| 2.24 | 25 | 10 | 2.4 | 2.2 | 43[f] | 0.36 | 45 | 30 | 5.15 | 0.90 | 24 |
| 3.05 | 25 | 10 | 2.4 | 4.1 | 85.5[f] | 0.34 | 65 | 30 | 5.15 | 1.60 | 26.5 |
| 3.75 | 25 | 10 | 2.4 | *e* | 107[f] | 0.37 | 85 | 30 | 5.15 | 2.44 | 29.8 |
| 5.04 | 25 | 10 | 2.4 | *e* | 199[f] | 0.40 | 105 | 30 | 5.15 | 3.6[g] | 34.2 |
| 6.16 | 25 | 10 | 2.4 | *e* | 300[f] | 0.53 | 130 | 30 | 5.15 | 5.0[g] | 37.3 |
| 8.2 | 25 | 10 | 2.4 | *e* | 450[f] | 0.61 | 165 | 30 | 5.15 | 8.0[g] | 40.5 |
| | | | | | $\lambda$ = 410 nm | | | | | | |
| 0.40 | 37.5 | 80 | 5.75 | 0.60 | 27.1 | 0.31 | 25 | 75 | 3.6 | 0.211 | 21 |
| 0.37 | 25 | 54 | 5.75 | 0.36 | 26.0 | 0.30 | 20 | 75 | 3.6 | 0.192 | 18.8 |
| 0.36 | 20 | 54 | 5.75 | 0.27 | 21.4 | 0.290 | 15 | 75 | 3.6 | 0.141 | 18 |
| 0.346 | 15 | 54 | 5.75 | 0.24 | 21.0 | 0.275 | 10 | 75 | 3.6 | 0.128 | 16.6 |
| 0.33 | 10 | 54 | 5.75 | 0.19 | 20 | 0.275 | 10 | 75 | 3.6 | 0.128 | 16.9 |
| 0.34 | 37.5 | 100 | 3.6 | 0.346 | 22.9 | 0.27 | 5 | 75 | 3.6 | 0.083 | 15.2 |
| | | | | | $\lambda$ = 355 nm | | | | | | |
| 0.39 | 25 | 6.75 | 0.9 | 0.061 | 4.44 | 6.83 | 25 | 6.75 | 0.9 | *e* | 173[f] |
| 0.76 | 25 | 6.75 | 0.9 | 0.114 | 5.54 | 3.1 | 175 | 13 | 3.13 | *e* | 165[f] |
| 1.23 | 25 | 6.75 | 0.9 | 0.215 | 7.75 | 3.0 | 175 | 13 | 2.5 | *e* | 124[f] |
| 1.95 | 25 | 6.75 | 0.9 | 0.384 | 15 | 2.84 | 175 | 13 | 2.0 | *e* | 103[f] |
| 2.77 | 25 | 6.75 | 0.9 | 0.838 | 28[f] | 2.78 | 175 | 13 | 1.5 | *e* | 96[f] |
| 4.15 | 25 | 6.75 | 0.9 | *e* | 29[f] | 2.73 | 175 | 13 | 1.0 | *e* | 74[f] |
| 5.66 | 25 | 6.75 | 0.9 | *e* | 110[f] | 2.83 | 175 | 13 | 0.5 | *e* | 59[f] |

[a] Solvent HOAc, 25 °C, path length 2 mm. [b] Calculated from the measured concentration $[H_2O]$ by using the formula $Y = \{H_2O\}/[H_2O] = 0.887 + 5.52/(3.11 + [H_2O]/M)$ deduced from the graph in ref 6. [c] Calculated as $k^0 = S_0/\Delta\epsilon l$ (see text and eq 15), with value of $S_0$ directly measured from the linear portion of an absorbance–time plot and $\Delta\epsilon = 7.81 \times 10^3$ and $2.81 \times 10^4$ $M^{-1}$ $cm^{-1}$ at $\lambda$ = 410 and 355 nm. [d] Calculated as $k^1 = 2S_0/B$, from values of $S_0$ and $B$ obtained by fitting $(dA/dt)$ to eq 14. [e] $k^0$ not obtained since the initial part of the absorbance–time curve is not sufficiently linear (see text; cf. Figure 4). [f] Obtained from a plot of log $(A - A_\infty')$ against time (see text; cf. Figure 6). [g] Calculated as $k^0 = S_0/\Delta\epsilon l$, with $S_0$ obtained as in footnote *d*.

reaction 2, i.e. whether this step is outer sphere or inner sphere. In experiments with zero initial iodide concentration, the absorbance first rapidly increased and then decreased. At low initial iodine concentration, and under conditions where the reaction is pseudo zero order, both increase and decrease were approximately linear with time (see Figure 11). The absorbance–time profile in fact closely resembles a "Job plot" for mixtures of $I_2$ and NaI, with the condition $[I_2] + {}^1/_2[NaI]$ = constant, and the maximum absorbance agrees well with the value calculated on the assumption that all the iodide is present as $NaI_3$, and not bound to chromium (Figure 11). In similar experiments with higher initial iodine concentration, the absorbance–time curves were similar except for a positive curvature near $t = 0$. This is consistent with catalysis by liberated iodide ion, i.e. step 2 of the mechanism (equation 2 above) consisting of parallel reaction paths

$$Cr^{II} + I_2 \rightarrow \text{products} \quad (20)$$

$$Cr^{II} + NaI_3 \rightarrow \text{products} \quad (21)$$

We have not pursued these measurements, however; we merely conclude that at least 90% of the iodide ion is released within about 1 s.

## Discussion

The limiting second-order iodide dependence of $k_1$ at high iodide concentration is consistent with a mechanism in which the dimer forms a diiodide adduct before dissociation

$$Cr_2(OAc)_4 + 2NaI \overset{K}{\rightleftharpoons} Na_2[Cr_2(OAc)_4I_2] \quad (22)$$

$$Na_2[Cr_2(OAc)_4I_2] \xrightarrow{k_1'} 2Na[Cr(OAc)_2I] \quad (23)$$

(13) Alternative expressions are, when $[H_2O] \simeq 0.4$ M, $k_1 \propto [H_2O]^{1.8}$ and $k_2^* \propto [H_2O]^{0.17}$; and when $[NaI] \simeq 0.025$ M, $k_1 \propto [NaI]^{1.14}$ and $k_2^* \propto [NaI]^{0.25}$.

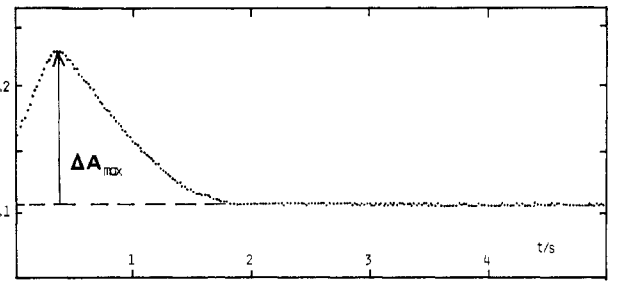


**Figure 11.** Absorbance–time plot for reaction in the absence of added NaI. ($[I_2]_0$ = 0.2 mM, $[Cr^{II}_2]_0$ = 3.6 mM, λ = 410 nm, path length 2 mm, $T$ = 25 °C). The maximum in the absorbance is attributed to a maximum in the concentration of $I_3^-$ ion, occuring when $[I_2]_T = [I^-]_T = {}^2/_3[I_2]_0$ = 0.4 mM. From $K = 2.2 \times 10^4$ $M^{-1}$ and measured extinction coefficients of the components, the value of $\Delta A_{max}$ is calculated as 0.116 compared with the measured value of 0.123.

where $k_1 = Kk'_1$. Presumably, the iodide ions are coordinated in the two axial positions, but the positions of the two sodium ions cannot be specified. The limiting first-order iodide dependence of $k_2$* is consistent with these steps, assuming that the subsequent reaction of the monomer is not catalyzed by iodide.

$$Na[Cr(OAc)_2I] + NaI_3 \xrightarrow{k'_2} Cr(OAc)_2I + NaI + NaI_2 \quad (24)$$

$$Na[Cr_2(OAc)_2I] + NaI_2 \rightarrow Cr_2(OAc)_2I + 2NaI \quad (25)$$

$$Cr(OAc)_2I \rightarrow \text{products} \quad (26)$$

Here, "$NaI_2$" denotes the sodium ion pair of the radical ion $I_2^-$, so that eq 24 and 25 together constitute the two-step mechanism that is usually postulated for reactions of one-electron reductants with $I_2$.[14,15] Equation 26 covers a number of steps, but in particular it involves the early release of iodide ion and polymerization of chromium(III) monomer to form a derivative of the oxo-centered trimer, such as $[Cr_3O(OAc)_6(HOAc)_3](OAc)$.

**Acknowledgment.** Equipment for this study was provided by the Science and Engineering Research Council and the Royal Society. L.M.W. thanks the SERC for a Research Studentship.

**Registry No.** $Cr_2(OOCCH_3)_4$, 15020-15-2; $I_2$, 7553-56-2.

(14) Woodruff, W. H.; Margerum, D. W. *Inorg. Chem.* **1974**, *13*, 2578.
(15) Rudgewick-Brown, N.; Cannon, R. D. *J. Chem. Soc., Dalton Trans.* **1984**, 479.

Contribution from the Department of Chemistry, California State University, Los Angeles, California 90032

# Net Front-Side Displacement Reactions in a Carborane System: Halide-Exchange Reactions among Derivatives of *closo*-2,4-Dicarbaheptaborane, 2,4-$C_2B_5H_7$

BRADFORD NG, THOMAS ONAK,* and KEITH FULLER

*Received April 4, 1985*

Halogen exchange is observed between *B*-halo derivatives of *closo*-2,4-$C_2B_5H_7$ and tetraalkylammonium halides and appears possible only when the "reagent" halide ion is smaller than the "leaving" halide. Thus, both 3- and 5-$IC_2B_5H_6$ react with bromide ion to give quantitative amounts of the respective 3- and 5-$BrC_2B_5H_6$ isomers. Similarly, 5-$BrC_2B_5H_6$ is converted to 5-$ClC_2B_5H_6$ in the presence of $Cl^-$. This same halide ion reacts with the carborane adduct $(CH_3)_3N$·5,6-$Br_2C_2B_5H_5$ to give both 5-Cl-6-$BrC_2B_5H_5$ and 5,6-$Cl_2C_2B_5H_5$. Fluoride ion reacts with 5-$BrC_2B_5H_6$ or with the trimethylamine adduct of 5-$ClC_2B_5H_6$ to give 5-$FC_2B_5H_6$. Two other fluorine-substituted carboranes, 3-$FC_2B_5H_6$ and 3,5-$F_2C_2B_5H_5$, are produced in yields exceeding 90% from tetrabutylammonium fluoride and 3-I and 3,5-$I_2$ derivatives of $C_2B_5H_7$, respectively. All indications point to an increase in (cage)-boron–halogen bond energy as the primary driving force behind the displacement reactions. The rate of substitution, as the halide ion is varied, is in correspondence with the expected nucleophilicity trend $F^- > Cl^- > Br^-$ in nonaqueous solvents. Halogen exchange in a few instances results in rearrangement products; i.e., both $(CH_3)_3N$·5-$IC_2B_5H_6$/benzyltriethylammonium bromide/$CH_2Cl_2$ and $(CH_3)_3N$·5-$IC_2B_5H_6$/benzyltriethylammonium chloride/$CH_2Cl_2$ mixtures produce substantial quantities of 3-$ClC_2B_5H_6$ below 100 °C.

## Introduction

Synthetic routes to B-substituted compounds of *closo*-2,4-$C_2B_5H_7$ have often involved the use of a Lewis acid to catalyze the introduction of the substituent[1-5] in a manner that is reminiscent of a Friedel-Crafts type of reaction. Several other reactions leading to *B*-X-2,4-$C_2B_5H_6$ compounds from the parent 2,4-$C_2B_5H_7$ are thermally induced or light-induced.[1,4-8] In addition, trace yields of three mono- and some difluoro derivatives of 2,4-$C_2B_5H_7$ are obtained from the direct action of $F_2$ on the parent carborane.[9] Also, another type of reaction leading to B-substituted dicarbaheptaboranes involves the removal of $Cl^-$ from 1:1 trimethylamine adducts of both 3-Cl- or 5-Cl-2,4-$C_2B_5H_6$, producing the respective $[B$-$(CH_3)_3N$·*closo*-2,4-$C_2B_5H_6]^+$ cation isomers.[10]

A previous study,[11] describing the surprising quantitative conversion of the trimethylamine adduct of 5-Br-2,4-$C_2B_5H_6$ in dichloromethane solution to the halogen exchange product, 5-Cl-2,4-$C_2B_5H_6$, provided the motivation for the present study. A mechanism was proposed in which a $[5$-$(CH_3)_3N$·*closo*-2,4-$C_2B_5H_6]^+$ intermediate combined with chloride ion (available from

(1) Warren, R.; Paquin, D.; Onak, T.; Dunks, G.; Spielman, J. R. *Inorg. Chem.* **1970**, *9*, 2285–2287.
(2) Olsen, R. R.; Grimes, R. N. *J. Am. Chem. Soc.* **1970**, *92*, 5072–5075.
(3) Ditter, J. F.; Klusmann, E. B.; Williams, R. F.; Onak, T. *Inorg. Chem.* **1976**, *15*, 1063–1065.
(4) Takimoto, C.; Siwapinyoyos, G.; Fuller, K.; Fung, A. P.; Liauw, L.; Jarvis, W.; Millhauser, G.; Onak, T. *Inorg. Chem.* **1980**, *19*, 107–110.
(5) Abdou, Z. J.; Soltis, M.; Oh, B.; Siwap, G.; Banuelos, T.; Nam, W.; Onak, T. *Inorg. Chem.* **1985**, *24*, 2363–2367.
(6) Onak, T.; Fung, A. P.; Siwanpinyoyos, G.; Leach, J. B. *Inorg. Chem.* **1979**, *18*, 2878–2882.
(7) Plotkin, J. S.; Astheimer, R. J.; Sneddon, L. G. *J. Am. Chem. Soc.* **1979**, *101*, 4155–4163.
(8) Oh, B.; Onak, T. *Inorg. Chem.* **1982**, *21*, 3150–3154.
(9) Maraschin, N. J.; Lagow, R. J. *Inorg. Chem.* **1975**, *14*, 1855–1859.
(10) Siwapinyoyos, G.; Onak, T. *Inorg. Chem.* **1982**, *21*, 156–163.
(11) Fuller, K.; Onak, T. *J. Organomet. Chem.* **1983**, *249*, C6–C8.

0020-1669/85/1324-4371$01.50/0 